Joint PIV&DSPI compared to standard Stereo PIV: some results from a turbulent boundary layer

J. Lobera, M. P. Arroyo
* Dpto. Física Aplicada. Facultad de Ciencias. Universidad de Zaragoza
C/ Pedro Cerbuna, 12, 50009- Zaragoza. SPAIN.

N. Perenne, M. Stanislas
** LML URA 1441, Bv. Paul Langevin, Cité Scientifique
59655-Villeneuve d'Ascq. FRANCE

e-mail: arroyo@posta.unizar.es

ABSTRACT

PIV&DSPI as a 3-C velocimetry technique has been set up to observe the turbulent boundary layer in a wind tunnel flow. Simultaneous stereo PIV recordings have been taken as a way to evaluate the performance of PIV&DSPI. For a mean velocity U=3 m/s and a magnification M=0.15, time intervals of 2 μs and 100 μs were used for DSPI and PIV recordings respectively. Angular stereo geometries with cameras on each side of the light sheet were used for both stereo PIV and PIV&DSPI. The recording geometry was obtained from the analysis of several calibration grid images. Spatial phase shifting (SPS) was included in the DSPI setup. The comparison of two recordings by means of a FFT based method produces a wrapped phase map (fig. 1a), with all the phase values contained between 0 and 2π. This image provides qualitative information on the spatial pattern of the out-of-plane velocity component, overlapped with a finite reference fringe system introduced by a slight misalignment of the laser beams. The phase map is unwrapped and the speckle noise is removed with a regularized phase tracking (RPT) technique so that absolute phase values are known. The finite reference fringe system is inferred from DSPI recordings taken when U=0 and subtracted from the flow unwrapped phase map so that only the contribution of the turbulent boundary layer flow is left. The unwrapped phase map (fig. 1b), shown wrapped for a better visualization, is an iso-contour plot for the out-of-plane velocity component. From the 2-C velocity data measured with PIV and the unwrapped phase map, the 3-C velocity data are obtained: they are plotted in figure 1c where the vector field represents the in-plane components (after subtraction of the mean velocity) while the isocontour map represents the out-of-plane component. These PIV&DSPI data agree well with the data measured with stereo PIV (fig. 1d).
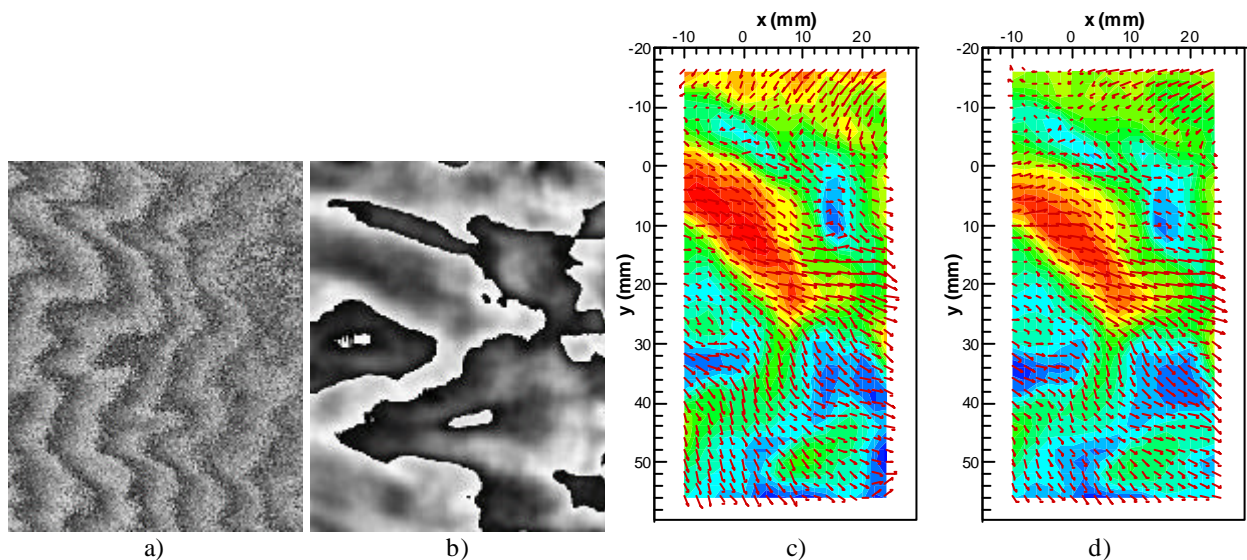
Fig. 1. PIV&DSPI results from a turbulent boundary layer flow. a) Wrapped phase map for U = 3m/s, as obtained from DSPI recordings; b) Unwrapped phase map from the processing of figure 1a, it shows the spatial pattern of the out-of-plane velocity; c) 3-C velocity data from PIV&DSPI; d) 3-C velocity data from stereo PIV.

1. INTRODUCTION

Stereo PIV (Prasad, 2000) is a quite well established technique for 3C-2D velocity field measurements. Stereo PIV requires a wider optical access than 2C PIV and suffers from an intrinsic lower accuracy in the out-of-plane velocity component measurements when the optical access gets narrower. Digital Speckle Pattern Interferometry (DSPI) as a fluid velocimetry technique (Andrés et al., 1999 & 2001, Arroyo et al., 2000) shares with 2C PIV the geometry for illumination and observation but is intrinsically sensitive to the out-of-plane component. Thus, the combination of DSPI with PIV should allow measuring the 3C-2D velocity fields from a common observing window and with a good accuracy for each of the three components. The main drawback for this PIV&DSPI combination is that DSPI is about two orders of magnitude more sensitive than PIV; thus, DSPI requires time intervals about two orders of magnitude smaller than the time intervals used for PIV. For slow flows, PIV&DSPI can be implemented with only one laser and one camera that records three separate frames. However, two cameras and a three cavity pulsed laser are necessary for high speed flows. DSPI also imposes requirements on some laser properties such as coherence length and beam divergence, which are not essential for PIV.

The works mentioned above report the set up of DSPI in a slow convective flow with a He-Ne laser and in a wind tunnel flow with a pulsed Nd-YAG laser and fiber optics. They all show good quality interferograms, which give qualitative information on the spatial pattern of the out-of-plane velocity component, using a 90° recording geometry but they do not present any quantitative data. This paper reports on the ability of DSPI for producing quantitative data, based on some experiments carried out at Laboratoire de Mécanique de Lille (LML) where measurements were simultaneously taken with PIV&DSPI and with stereo PIV in a wind tunnel turbulent boundary layer. In the following, the experimental techniques are described and some quantitative results are presented. The accuracy of the PIV&DSPI data is estimated by comparison with the stereo PIV data.

2. EXPERIMENTAL TECHNIQUES

2.1 The flow

The experiments presented in this paper have been carried out in the LML wind tunnel. This wind tunnel has a cross section of 1 m x 2 m; the freestream velocity was set to 3 m/s. The Reynolds number, based on momentum thickness, is 5500. The boundary layer is turbulent. A plane perpendicular to the wall and parallel to the main velocity was illuminated. A 40x75 mm^2 section of the boundary layer near the windtunnel top wall was recorded. The whole flow was seeded with oil particles.

2.2 Optical setup

The beam coming from a four independent cavity Nd-YAG pulsed laser is shaped into a light sheet that illuminates an XY plane (Figure 2). Four PCO Sensicam PIV cameras were set to observe the upper part of the light plane. Camera 1 and 2, symmetrically looking at an angle of 45° from opposite sides of the light sheet, were used for the stereo PIV recordings. Camera 3 and 4, also symmetrically looking from opposite sides of the light sheet but at an angle of 25° with the light sheet, were used for the PIV&DSPI recordings. Camera 3 was used for PIV while camera 4 was used for DSPI. In all cases, an angular arrangement was used; Scheimpflug adapters specially designed by LML were used to properly align each CCD sensor and its corresponding recording lens. The laser energy was set to 60 mJ/pulse; MicroNikkor 105 mm lenses with f/11 were used for cameras 1 and 2 while Nikon 120 mm lenses with f/16 and f/22 were used for cameras 3 and 4 respectively.

The synchronization of lasers and cameras was done using Lavision hardware and software, specially adapted for these experiments. DSPI used the third and four pulses, which come from two injection seeded cavities and whose overlapping and divergence were carefully optimized. The two pulses, fired at a time interval of 2 μs, were recorded in two separate frames of camera 4; at the same time, they were also recorded together on the second frame of cameras 1, 2 and 3. The first frame of these three cameras recorded the first and second pulses, which were simultaneously fired from two unseeded cavities and whose overlapping was carefully optimized. The time interval between the first and the third pulses was set to 100 μs.

DSPI, as an interferometric technique, requires a reference beam that must be superposed with and recorded at the same time as the object beam (light scattered by the particles in the illuminated fluid plane). Camera 4 was adapted for DSPI by placing a small rail where a mirror, a divergent lens and a beamsplitter cube (acting as a beam combiner) were set for the reference beam arm. A small part of the main laser beam was diverted and sent to this arm to form the reference beam, whose energy was adjusted by means of a three linear polarizer system, PL, acting as a continuously variable neutral density filter.
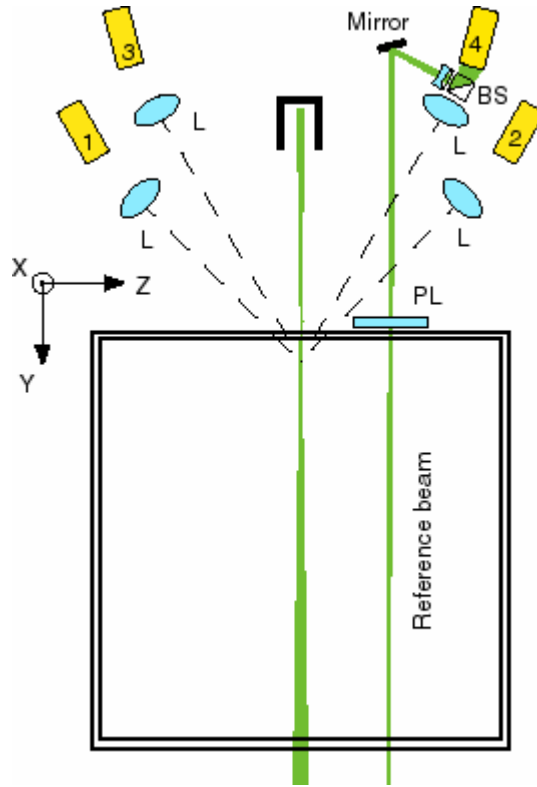
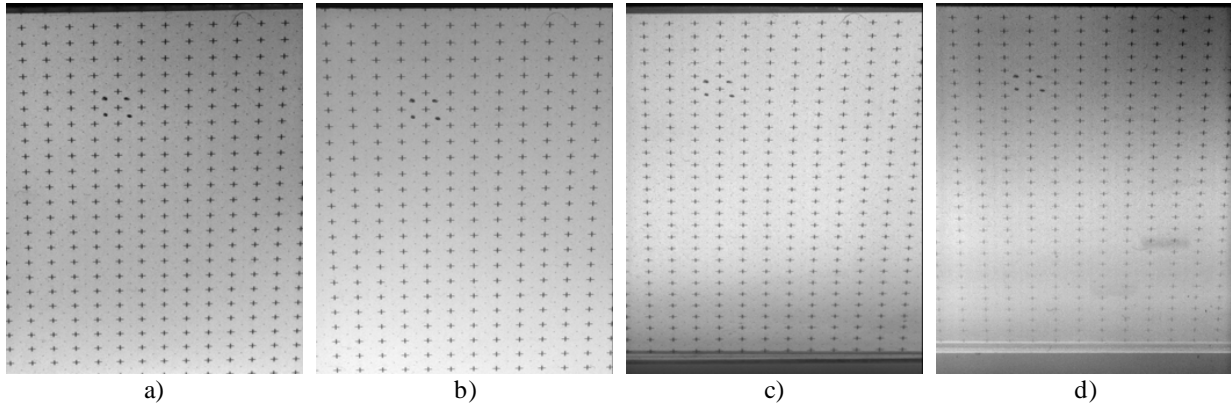Fig. 2. Stereo PIV and PIV&DSPI optical setup.

a)   b)   c)   d)

Fig. 3. Calibration grids as recorded from: a) camera 1; b) camera 2; c) camera 3; d) camera 4.

2.3 Stereo PIV analysis

In the present experiments a 3-d calibration based reconstruction following Soloff et al. (1997) was used to map the 2-C displacements measured from each camera to the real object space and for combining them to obtain the three-dimensional data. The calibration target is a Cartesian grid of black crosses on a transparent background; the spacing of the grid is 3.4 mm. One cross is surrounded by four dots and is used as the coordinate origin. The target plate is placed in the light sheet and viewed by the four cameras; the cameras are aligned by optimizing the overlapping of the region recorded by all of them. The calibration grid images recorded by each camera (figure 3) shows very good overlapping for camera 1 and 2 and for camera 3 and 4, but there is a small displacement in the field of view in the X direction between the two camera pairs. The calibration grid images were taken using a white light source to illuminate the target and a maximum aperture for all the lenses (f/2.8 for the MicroNikkor 105 mm lenses and f/5.6 for the Nikkon 120 mm). Eight more calibration images were recorded displacing the target from z = -2.0 mm to z = -2.0 mm with a 0.5 mm separation between two consecutive images.

For each camera, five calibration images were used to obtain the relationship between the three-dimensional object field position (in mm) and its corresponding two dimensional image field position (in pixels) by means of a polynomial

expression like in Soloff et al. (1997). We also used, following Willert 1997, a direct mapping of the particle images recorded at the same time by the four cameras into particles in the object plane as a way to check that the overlapping between the calibration target and the light sheet was good.

The stereo PIV analysis is done in the following way. First of all, a Cartesian grid in the object space is defined. In the second step, the position in the image space for camera 1 and camera 2 is calculated using the mapping function from the 3-D calibration (for z=0). The third step consists in interrogating the particle image fields according to the mapped grid in each camera so that two 2-C displacement fields are obtained. This 2C-PIVanalysis is performed using a single pass with 64x64 pixel interrogation windows, 3-point-Gaussian-peak-fitter and no post-processing. Finally, the three-dimensional displacements are determined using again the mapping function as suggested by Soloff et al. (1997). In this way, the 3-C vector field in a Cartesian grid is determined without any need for interpolation.

2.4 Digital Speckle Pattern Interferometry, DSPI

Since DSPI as a velocimetry technique is not widely known, let us recall first some basic concepts. The recorded images in DSPI are not particle fields but speckle fields (that can be called specklegrams) obtained as the interference between a particle image field (object beam) and a uniform reference beam. The particle displacement changes the object beam phase, which produces a change on the local speckle intensity. The phase change at a given point of the object plane is given by (Jones and Wykes, 1989)

$$\Delta\phi = \mathbf{K} \cdot \mathbf{d} \qquad\qquad (1)$$

where $\mathbf{d}$ is the displacement vector, $\mathbf{K} = (2\pi/\lambda)\,(\mathbf{u_o}\text{-}\mathbf{u_i})$ is the sensitivity vector $\mathbf{u_o}$ and $\mathbf{u_i}$ being the unity vectors in the observation and illumination directions respectively. Thus measuring $\Delta\phi$ will give information about d_k, the projection of $\mathbf{d}$ along $\mathbf{K}$. In fluid velocimetry, $\mathbf{K}$ always has an out-of-plane component and thus DSPI will give information about $\mathbf{d}$ which is complementary to the information provided by PIV, even when the two cameras look at the fluid plane from the same direction. In the present experiments the PIV&DSPI cameras were arranged in a stereoscopic configuration only because of compatibility with the stereo PIV setup. Because camera 4 is looking at the fluid plane with a small angle (25°), $\mathbf{K}$ is almost perpendicular to the fluid plane and thus DSPI is mainly sensitive to the out-of-plane velocity component.

In DSPI, the two specklegrams are recorded in separate frames and the $\Delta\phi$ is calculated from them. As a first approach, the absolute intensity difference between the two specklegrams (Andrés et al., 1999) produces a fringe pattern (that can be called interferogram) where $\Delta\phi$ can be determined from the local fringe intensity. The same type of interferogram, but with better quality, can be obtained by calculating the local speckle correlation coefficient for the two specklegrams (Schmitt and Hunt, 1997; Andrés et al., 2001). However, the most accurate determination of $\Delta\phi$ is obtained when Spatial Phase Shifting techniques, SPS (Burke, 2001; Robinson and Reid, 1993) are used.

SPS requires a finer control over the object and reference beam overlapping so that a modulation in the intensity for each speckle in the specklegram is produced. This modulation allows to calculate the phase (modulus 2π) of each speckle in each specklegram. As a first approach, a local three pixel intensity calculation can be used to determine this phase (Robinson and Reid, 1993). Here, we have used a Fourier transform method, FTM (Takeda et al., 1982; Saldner et al., 1996) which is more robust. This is specially noticeable when the reference beam is not perfectly uniform as in the present experiments; this is a common situation when Nd-YAG lasers are used.

In SPS-DSPI, $\Delta\phi$ (modulus 2π) is obtained from the subtraction of the local phase for the two specklegrams. By mapping $\Delta\phi$ as intensity values, a wrapped phase map is produced. The wrapped phase map (see Figure 5a) looks like an isocontour map for d_K. For any quantitative determination, absolute phase values are needed, i.e. the phase map has to be unwrapped and the speckle noise removed. A Regularized Phase Tracking, RPT, algorithm (Servin et al., 1999) is used for this purpose.

2.5 PIV&DSPI analysis

The PIV&DSPI analysis is done in the following way. First of all, a Cartesian grid in the object space is defined, as in stereo PIV. In the second step, the position in the image space for camera 3 and camera 4 is calculated using the mapping function from a 3-D calibration (for z=0) obtained as in stereo PIV. The third step consists in interrogating the particle image fields according to the mapped grid in camera 3 so that one 2-C displacement field is determined. In the fourth step, the unwrapped phase map is calculated. The absolute phase values are known for all the image plane points, however only the phase values on the mapped grid in camera 4 are used for the three-dimensional analysis. Three equations are obtained using the mapping function of Soloff et al. (1997) for the PIV data and equation (1) for the DSPI data. Equation (1) needs the knowledge of the recording geometry. The mapping function for camera 4 is

used to determine this geometry. The three dimensional displacements are determined by solving one set of three equations for each point of the grid.

3. 3-C VELOCITY RESULTS

The Cartesian grid in the object space has been chosen to cover the area common to the four camera images. The constant grid spacing of 2 mm in object space varies between 30 and 50 pixels in image space. Figure 4 shows the 2-C displacement fields determined from the PIV records taken with cameras 1 to 3. They are plotted such that the X-axis goes from left to right and the Y-axis from top to bottom (as in the calibration grids shown in figure 3 and in all the subsequent images). The vectors represent the 2-C displacement with a scale common to the three images. The isocontour maps correspond to the vertical (stereoscopic component) displacement; the color coding is common for the three images. The fields from camera 1 and 2 show noticeably different displacement values, which is necessary for stereo PIV to work properly. The fields from camera 1 and 3 are not only similar in the spatial pattern but also in the displacement values thus confirming that stereo PIV will not work properly with those cameras.
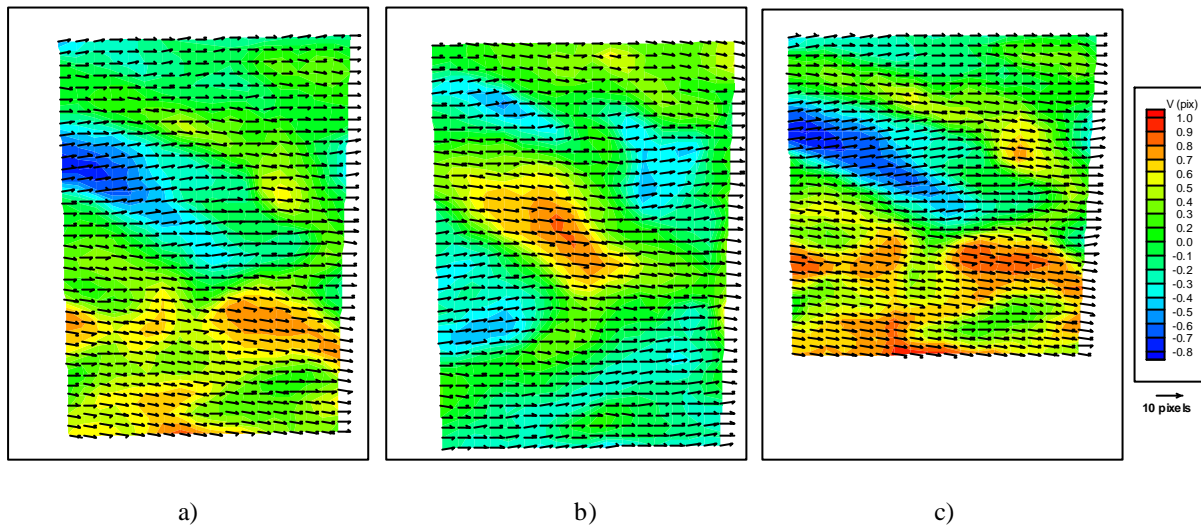

a)   b)   c)

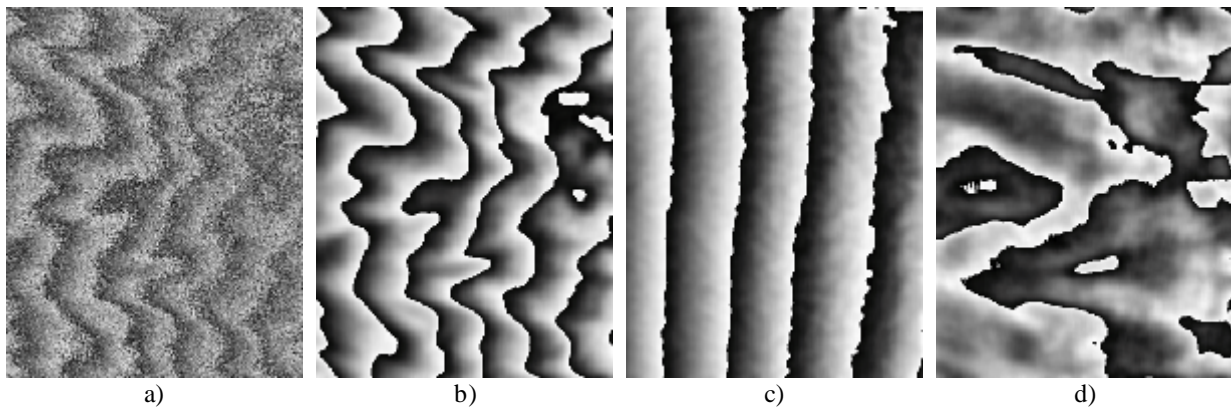Fig. 4. 2-C displacement fields as measured from: a) camera 1; b) camera 2; c) camera 3.

a)   b)   c)   d)

Fig. 5. SPS-DSPI results. a) Wrapped phase map for U=3m/s, WPF; b) Unwrapped phase map from figure 5a, UPF;
c) Unwrapped phase map for U=0, UP0; d) Unwrapped phase map corresponding to the flow, UPF-UP0

Figure 5 shows the information obtained with SPS-DSPI. The wrapped phase map, WPF, directly obtained from two consecutive SPS-DSPI records taken with camera 4 and analyzed with the Fourier transform method is shown in figure 5a. The unwrapped phase map, UPF, is obtained by applying the RPT algorithm on WPF; UPF (figure 5b) is shown wrapped for a better visualization and it contains information on the absolute phase change, i.e. on the velocity field, in every pixel of the recorded image. The unwrapped phase map shown in figure 5c, UP0, was obtained from two specklegrams recorded when U=0. This "finite reference fringe system" is produced by an angular misalignment between the reference beams for laser pulses 3 and 4. This finite reference fringe system is removed

from UPF by subtracting the two phase maps so that only the contribution of the flow is left (Figure 5d). The image on figure 5d represents an iso contour map for the out-of-plane velocity component.

Figure 6 shows the 3-C velocity measurements obtained with stereo PIV (figure 6a) and with PIV&DSPI (figure 6b). Data from cameras 1 and 2 were used for the stereo PIV measurements while data from camera 3 and 4 were used for the PIV&DSPI measurements. Both sets of data agree pretty well. The advantage of PIV&DSPI is that the 3-C data can also be obtained with good accuracy from any pair of cameras; we have checked that camera 1 and 4 and 2 and 4 also give good 3-C measurements
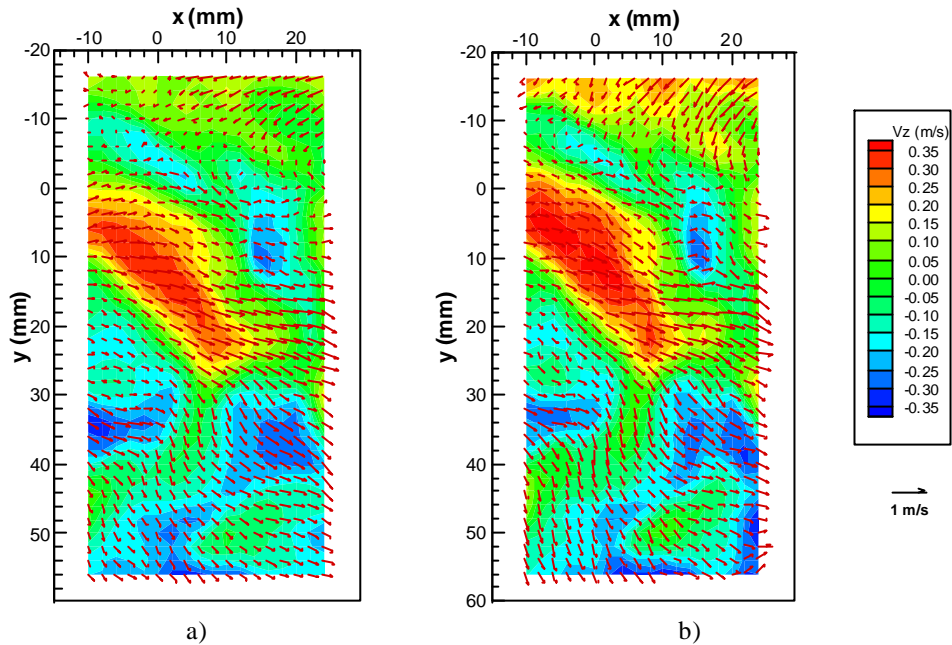
Fig. 6. 3-C velocity measurements; the vectors field represents the in-plane components (after substraction of the mean velocity) while the isocontour map represent the out-of-plane component. a) Data from stereo PIV; b) Data from PIV&DSPI.

4. CONCLUSIONS

We have shown that it is possible to implement DSPI in a wind tunnel and get quantitative data even in turbulent flows. Optical fibers are not needed in the reference beam but good control over the laser beam geometrical characteristics is necessary. The 3-C velocity data obtained with PIV&DSPI agrees well with the stereo PIV data; however, PIV&DSPI requires less optical access than stereo PIV. The combination PIV&DSPI can be set in a stereo configuration like in the present experiments or in a non stereo configuration, as shown in previously published papers (Andrés et al. 1999 & 2001). The SPS techniques are essential in obtaining quantitative data with DSPI.

REFERENCES

Andrés, N., Arroyo, M.P., Hinrichs, H. and Quintanilla, M. (1999). "Digital speckle pattern interferometry as full field fluid velocimetry technique", Opt. Lett., 24, pp. 575-577.

Arroyo, M.P., Andrés, N. and Quintanilla, M. (2000). "The development of full field interferometric methods for fluid velocimetry.", Opt. and Laser Technol., 32, pp. 535-542.

Andrés, N., Arroyo, M.P., Zahn, H. and Hinrichs, H. (2001). "Application of digital speckle pattern interferometry for fluid velocimetry in wind tunnel flows", Exp. in Fluids, 30, pp. 562-567.

Burke, J. (2001). "Application and optimisation of the spatial phase shifting technique in digital speckle interferometry" Thesis work, University of Oldenburg, Shaker Verlag, Aachen.

Jones, R. and Wykes, C. (1989). "Holographic and speckle interferometry", chap 3, Cambridge University Press, Cambridge.

Prasad, A.K. (2000). "Stereoscopic Particle Image Velocimetry", Exp. in Fluids, 29, pp. 103-116.

Robinson, D. W. and Reid, G. T. eds., (1993). "Interferogram Analysis", IOP, Bristol.

Saldner, H., Molin, N. and Stetson, K. (1996). "Fourier-transform evaluation of phase data in spatially phase-biased TV holograms", Appl. Opt., 35, pp. 332-336.

Servín, M., Cuevas, F. J., Malacara, D., Marroquin, J. L. and Rodriguez-Vera, R. (1999). "Phase unwrapping through demodulation by use of the regularized phase-tracking technique", Appl. Opt., 38, pp. 1934-1941.

Soloff, S.M., Adrian, R.J. and Liu, Z.C. (1997). "Distortion compensation for generalized stereoscopic particle image velocimetry", Meas. Sci. Technol., 8, pp. 1441-1454.

Takeda, M., Ina, H. and Kobayashi, S. (1982). "Fourier-transform method of fringe-pattern analysis for computer-based topography and interferometry", J. Opt. Soc. Am., 72, pp. 156-160.

Willert, C. (1997). "Stereoscopic digital particle image velocimetry for application in wind tunnel flows", Meas. Sci. Technol., 8, pp. 1465-1479.